Airborne particulate matter ($PM_{2.5}$) triggers ocular hypertension through pyroptosis

Liping Li
Fudan University Eye Ear Nose and Throat Hospital https://orcid.org/0000-0002-0257-0037
Chao Xing
Fudan University Eye Ear Nose and Throat Hospital
Liangliang Niu
Fudan University Eye Ear Nose and Throat Hospital
Bin Luo
Lanzhou University
Ji Zhou
Shanghai Meteorological Bureau
Maomao Song
Fudan University Eye Ear Nose and Throat Hospital
Jingping Niu
Lanzhou University
Ye Ruan
Lanzhou University
Xinghuai Sun
Fudan University Eye Ear Nose and Throat Hospital
Yuan Lei (lilian0167@hotmail.com)
Fudan University Eye Ear Nose and Throat Hospital

Research

Keywords: PM2.5, NLRP3, intraocular pressure (IOP), human trabecular meshwork cell (HTM), pyroptosis

Posted Date: January 19th, 2021

DOI: https://doi.org/10.21203/rs.3.rs-75533/v1

Version of Record: A version of this preprint was published at Particle and Fibre Toxicology on March 4th, 2021. See the published version at https://doi.org/10.1186/s12989-021-00403-4.

Abstract

Background Particulate matter (PM) is strongly linked to human health and has detrimental effects on the eye. Studies have, however, focused on the ocular surface, with limited research on the impact of $PM_{2.5}$ on intraocular pressure (IOP).

Methods To investigate the impact of $PM_{2.5}$ on IOP and the associated mechanism, C57BL/6 mouse eyes were topically exposed to a $PM_{2.5}$ suspension for 3 months, and human trabecular meshwork (HTM) cells were subjected to various $PM_{2.5}$ concentrations *in vitro*.

Results The results revealed that the IOP increased gradually after $PM_{2.5}$ exposure, and an upregulation of NLRP3 inflammasome, caspase-1, IL-1β, and GSDMD protein levels was observed in outflow tissues. $PM_{2.5}$ exposure decreased HTM cell viability and affected contraction. Further, elevated ROS levels were observed as well as an activation of the NLRP3 inflammasome and downstream inflammatory factors caspase-1 and IL-1β. ROS scavenger or caspase-1 inhibitor treatment improved these $PM_{2.5}$-induced changes.

Conclusion This study provides novel evidence of the $PM_{2.5}$-mediated development of ocular hypertension, which occurs as a result of increased oxidative stress and the subsequent induction of pyroptosis in trabecular meshwork cells.

Highlights

- $PM_{2.5}$ exposure increases intraocular pressure accompanied by intraocular tissue pyroptosis
- $PM_{2.5}$ triggered oxidative stress which activated pyroptosis in human trabecular meshwork cells
- NLRP3 inflammasome mediates PM_5 induced trebecualr meshwork pyrotosis

Introduction

Epidemiological and experimental studies suggest that particulate matter (PM), especially $PM_{2.5}$ (aerodynamic diameter ≤ 2.5 μm), is strongly associated with respiratory, cardiovascular, metabolic, and even emotional disorders[1]. Although the eyes are in direct contact with the external environment, studies on the impact of $PM_{2.5}$ on ocular health remain scarce[2]. According to previous studies, PM causes ophthalmic diseases such as conjunctivitis, keratitis, and dry eye syndrome [3, 4, 5, 6]. However, these PM-associated studies focused on the ocular surface, with little consideration of the particles' potential to penetrate the human cornea and affect tissues within the eye, and their involvement in the initiation and development of intraocular disease.

It is possible that the recent increase in air pollution may be an important cause of, for example, glaucoma[7]. An epidemiological study, for the first time, presented a relationship between long-term air pollution and intraocular pressure elevation[7]. Other studies have demonstrated the association between

the $PM_{2.5}$ exposure and glaucoma, without any link to IOP elevation, but through neurotoxicity and vascular dysfunction in the retina[8, 9]. Therefore, conducting investigations to elucidate the link between the $PM_{2.5}$ and glaucoma as well as the associated underlying mechanisms is of relevance.

The production and outflow of aqueous humor dynamically maintain intraocular pressure (IOP). Outflow resistance is reported in the juxtacanalicular tissue (JCT) region, where adjacent trabecular meshwork (TM) and Schlemm's canal (SC) endothelial cells regulate aqueous humor outflow[10]. Cellular or extracellular stimuli such as oxidative stress can damage the TM, causing inflammation and cell death, thereby causing IOP elevation and, eventually, glaucoma[11, 12].

The aim of the current study was to investigate the association between $PM_{2.5}$ and ocular hypertension and to elucidate the mechanisms underlying this relationship. This study was incentivized by the unintentional discovery that topical application of fluorescent mock $PM_{2.5}$ to the eye caused deposition in outflow tissues including the iris, ciliary body, and TM. These tissues are vital for regulating aqueous humor outflow resistance and IOP[10]. The current findings suggest that, apart from its involvement in ocular surface disease, $PM_{2.5}$ pollution also affects tissues inside the eye, possibly participating in the development of intraocular diseases such as glaucoma.

Results

$PM_{2.5}$ exposure induced ocular hypertension in C57BL/6 mice

Elevated IOP values were observed in mouse eyes exposed to $PM_{2.5}$ from day 25 to 104. During this period, the average IOP elevation was 2.6 mmHg, with a maximum of 4.7 mmHg observed on day 92 ($n = 7$, $p < 0.05$, Figure 1A). From day 1 to day 24, IOP values for both eyes (treated and controls) were similar. On day 25, the IOP values of $PM_{2.5}$-treated eyes significantly increased relative to PBS-treated eyes (14.8 ± 0.6 mmHg, $n = 10$ vs 12.3 ± 0.8 mmHg, $n = 7$, $p < 0.05$). Elevated IOP was sustained for 3 days, followed by 2 days of normalization. Thereafter, IOP values increased again and remained consistently higher compared to values of control eyes. IOP elevation was steadily significant from day 30 onwards, with IOP values of 14.9 ± 1.4 mmHg and 12.4 ± 1.1 mmHg for $PM_{2.5}$-treated eyes and PBS-treated eyes, respectively (PBS treated, $n = 10$; $PM_{2.5}$-treated, $n = 10$; $p < 0.05$). Our data demonstrate that $PM_{2.5}$ exposure adversely affected IOP, thus representing a risk factor for glaucoma.

Characteristic features of pyroptosis in outflow tissues following $PM_{2.5}$ exposure

In order to understand the underlying mechanism of $PM_{2.5}$-related ocular hypertension, we measured the levels of proteins associated with the classic pyroptosis pathway (NLRP3/caspase-1/IL-1β/GSDMD) in aqueous humor outflow tissue (Figure 1B). NLRP3 expression increased 1.2-fold in outflow tissue of $PM_{2.5}$-treated eyes compared to that of control eyes ($n = 3$, $P < 0.05$). Further, levels of NLRP3 downstream proteins caspase-1 and GSDMD increased 3.1- and 6.3-fold, respectively ($n = 4$, $p < 0.05$). In addition, total IL-1β was 1.7 times higher in outflow from $PM_{2.5}$-treated eyes compared to contralateral

controls, whereas cleaved IL-1β increased 5.5-fold (n = 3, $p < 0.05$). These observations suggested that $PM_{2.5}$ caused tissue injury via pyroptosis of cells in outflow tissue of the eye.

To understand $PM_{2.5}$ entry into the anterior chamber, a fluorescent mock $PM_{2.5}$ tracer was topically applied to the eye. Particles with diameters from 10 to 500 nm passed through the cornea into the anterior chamber and were mainly deposited in outflow tissue, with ciliary body deposition being the most pronounced (Figure 1C). Fluorescent tracer distribution revealed that some $PM_{2.5}$ crossed the cornea and entered the eye, thereby affecting intraocular function.

$PM_{2.5}$ exposure triggered pyroptosis in HTM cells

To further verify the relationship between $PM_{2.5}$ and pyroptosis in order to explain the effect of $PM_{2.5}$ on IOP, we utilized HTM cells as an *in vitro* model. As previously mentioned, HTM cells are vital components of outflow tissue, which is the main site of outflow resistance and a key IOP determinant. We initially found that $PM_{2.5}$ was toxic to HTM cells even at 25 μg/mL. When HTM cells were exposed to different $PM_{2.5}$ concentrations for 48 h, a concentration-dependent decrease of cell viability was observed. HTM cell viability was reduced by 18.01%, 36.52%, 36.80%, 41.89%, and 47.71% after treatment with concentrations of 25, 50, 100, 200, and 400 μg/mL $PM_{2.5}$, respectively (n = 5 cell lines, $p \leq 0.05$, vs. controls groups, Figure 2A).

We further observed that NLRP3 protein levels were upregulated 2.7- and 1.6-fold after HTM cells were treated with 100 and 200 μg /mL of $PM_{2.5}$, respectively, for 48 h (n = 4 cell lines, $p < 0.05$, Figure 2B). RT-qPCR results revealed that 48 h of $PM_{2.5}$ exposure increased the relative expression of NLRP3 mRNA 1.3- and 1.4-fold in 100 μg/mL and 200 μg/mL $PM_{2.5}$-treated HTM cells (n = 3 cell lines, $p < 0.05$, Figure S1), respectively.

Moreover, the protein expression of caspase-1 increased by factors of 2.3 and 2.6 in $PM_{2.5}$-treated HTM cells compared to controls (100 μg/mL and 200 μg/mL, n = 3 cell lines, $p < 0.01$, Figure 2B). However, the relative expression of caspase-1 mRNA decreased 0.8-fold in $PM_{2.5}$-treated cells (100 μg/mL or 200 μg/mL, n = 3 cell lines, $p < 0.05$, Figure S1).

Activation of caspase-1 facilitates cleavage of GSDMD, release of the N-terminal GSDMD fragment, and maturation of IL-1β, leading to inflammatory cell death. Notably, in control cell supernatant, the average protein concentration of IL-1β was 12.13 ± 2.56 pg/mL, whereas in $PM_{2.5}$-treated cell culture supernatant, IL-1β levels of 20.42 ± 5.02 and 19.23 ± 5.06 pg/mL were observed after 100 and 200 μg/mL $PM_{2.5}$ treatment, respectively (n = 8 cell lines, $p < 0.05$, Figure 2B). IL-1β mRNA expression was also higher in $PM_{2.5}$-treated HTM cells compared with controls by factors of 15.0 and 15.4 for treatment concentrations of 100 and 200 μg/mL, respectively (n=6 cell lines, $p<0.05$, Figure S1). The protein expression of GSDMD increased by factors of 1.4 and 1.2 in $PM_{2.5}$-treated HTM cells compared to controls (100 μg/mL and 200 μg/mL, n = 3 cell lines, $p > 0.05$, Figure 2B).

To further characterize the $PM_{2.5}$-induced pyroptosis of HTM cells, we performed immunofluorescence staining for NLRP3 and caspase-1 after 100 μg/mL $PM_{2.5}$ exposure for 48 h. As can be seen in Figure 2D and E, NLRP3 and caspase-1 protein levels increased in $PM_{2.5}$-exposed HTM cells.

Taken together, these observations revealed the cellular and molecular mechanisms through which $PM_{2.5}$ increased IOP. $PM_{2.5}$ caused cellular toxicity and pyroptosis by activating NLRP3, caspase-1, and GSDMD. This suggests that pyroptosis is an important mediator of ocular cell damage and of the decreased cell viability induced by $PM_{2.5}$.

Increased ROS formation and enhanced HTM contraction following $PM_{2.5}$ exposure

Prior studies demonstrated that ROS elevation is essential for inflammasome activation[4, 13]. Therefore, in order to verify the role of ROS in $PM_{2.5}$-induced pyroptosis, we measured the changes of intracellular ROS levels in HTM cells after treatment with $PM_{2.5}$ (100 μg/mL) for 48 h. Representative micrographs of the DCF fluorescently-labeled cells indicate that the $PM_{2.5}$ elevated ROS in HTM cells (Figure 2F). Further, the contractility of $PM_{2.5}$-treated HTM cells increased 2.4-fold compared to controls after 48 h of treatment (Figure 2G), probably due to the increase in ROS levels. Combined with the results presented in Figure 2, it can be inferred that $PM_{2.5}$-related ROS formation likely reduced cell viability and caused pyroptosis. However, further pharmacological experiments are required to test this hypothesis.

Role of ROS and caspase-1 in $PM_{2.5}$-induced HTM cell pyroptosis

To further assess if $PM_{2.5}$-induced pyroptosis of HTM cells is triggered by ROS and dependent on caspase-1, we conducted ROS and caspase-1 inhibitory experiments. The ROS scavenger NAC and caspase-1 selective inhibitor VX-765 were tested for their potential in preventing/alleviating $PM_{2.5}$-induced cell damage. Figure 3A reveals that 48 h of $PM_{2.5}$ exposure lowered HTM cell viability by 24.7% ($n = 5$, $p < 0.05$), while pretreatment with NAC (3 mM) markedly reduced ROS formation in HTM cells (Figure S1) and increased cell viability by 40.0% ($n = 5$, $p < 0.$). Similarly, after VX-765 (100 μM) pretreatment, the viability of HTM cells exposed to $PM_{2.5}$ increased by 23.3% ($n = 5$, $p > 0.05$). NAC and VX-765 alone, however, had no effect on HTM cell viability, suggesting that the ROS scavenger and caspase-1 inhibitor may help prevent $PM_{2.5}$-induced cell damage.

Our results further demonstrate that NAC and VX-765 significantly downregulated the expression of the NLRP3, caspase1, GSDMD and IL-1β (Figure 3B and C). Figure 3D and E show that NAC inhibited NLRP3 and caspase-1 expression in $PM_{2.5}$-exposed HTM cells, and a distinct decrease in caspase-1 was observed in the HTM cells treated with VX-765 after $PM_{2.5}$ exposure (Figure 3E). This indicates that $PM_{2.5}$-induced HTM pyroptosis requires ROS and depends on caspase-1, and ROS scavenger or caspase-1 inhibitor pretreatment effectively reduces $PM_{2.5}$-induced injury.

Discussion

This is the first study to demonstrate that $PM_{2.5}$ exposure leads to ocular hypertension and glaucoma by inducing cell pyroptosis and inflammation in intraocular tissues responsible for controlling IOP. Reducing ROS production or inhibiting caspase-1 prevented $PM_{2.5}$-induced inflammation and pyroptosis of HTM cells.

Various eye diseases such as dry eye syndrome, conjunctivitis, and keratitis are attributed to air pollution, especially $PM_{2.5}$ pollution, according to epidemiological and experimental studies[14, 15, 16, 17]. $PM_{2.5}$ exposure is also linked to high blood pressure[18], a condition with a pathological mechanism resembling that of high intraocular pressure[19, 20]. For example, oxidative stress promotes vascular aging and damage, which contributes to hypertension[21]. Similarly, oxidative stress induces trabecular meshwork cell damage, which impairs aqueous humor drainage, thereby causing ocular hypertension[22]. However, $PM_{2.5}$ has not yet been reported as inducing ocular hypertension. Jama *et al.*, however, suggested that environmental black carbon exposure may represent a risk factor for increased intraocular pressure in individuals susceptible to other biological oxidative stressors. Consistent with Jama's study, we observed that topical application of a $PM_{2.5}$ suspension can cause ocular hypertension in mice (Figure 1A). Therefore, to the best of our knowledge, the relationship between $PM_{2.5}$ and intraocular pressure-related disease had remained unproven *in vivo*, and this study is the first to report the association of $PM_{2.5}$ with IOP changes in mice.

The classical pyroptosis pathway is central to $PM_{2.5}$-induced injury. Previous studies have reported $PM_{2.5}$-induced NLRP3 inflammasome activation and ocular injury *in vivo* and *in vitro*[15, 23, 24, 25, 26, 27, 28, 29, 30, 31]. The NLRP3 inflammasome is a vital component of sterile- and infection-triggered inflammation as well as of the immune responses to various diseases[32]. Classical pyroptosis is mediated by the NLRP3 inflammasome, and caspase-1 activation promotes the cleavage of pro-IL-1β and GSDMD[33]. Previous studies have revealed that NLRP3 inflammasome activation greatly contributes to cardiovascular, neurological, and lung disease development[25, 26, 27, 28, 29, 30, 31]. In addition, ROS have been reported to activate the NLRP3 inflammasome in environment-induced dry eye and conjunctivitis, and a significant increase of inflammatory factors, such as IL-1β, was observed.[14, 15, 16, 17] However, whether the NLRP3 inflammasome participates in PM-induced injury in outflow tissues has been poorly studied. Consistent with previous studies, our results revealed an increase of NLRP3 protein levels in outflow tissues of $PM_{2.5}$ topically-treated mouse eyes (Figure 2). We further demonstrated the $PM_{2.5}$-induced upregulation of the caspase-1, which indicates NLRP3 inflammasome activation. Increased IL-1β protein and cleaved IL-1β were also observed (Figure 1B). In addition, fluorescent $PM_{2.5}$ tracer experiments revealed that particles with diameters from 10 to 500 nm passed through the cornea, entered the anterior chamber, and finally settled in the ciliary body (Figure 1C). These findings suggest that the NLRP3/caspase-1/IL-1β axis is active in $PM_{2.5}$-induced ocular hypertension. Since trabecular meshwork tissue is vital for the regulation of IOP, and their damage is closely associated with increased aqueous outflow resistance and IOP elevation[34], we suggest that HTM cells undergo pyroptosis during $PM_{2.5}$-induced ocular hypertension.

Following results from mice, we observed $PM_{2.5}$-induced pyroptosis in HTM cells, which was consistent with observations in $PM_{2.5}$ topically-treated mouse eyes. First, we demonstrated that $PM_{2.5}$-mediate cell viability reduction was concentration-dependent (Figure 2A). When HTM cells were exposed to different $PM_{2.5}$ concentrations (25–400 μg/mL) for 48 h, their viability significantly decreased. $PM_{2.5}$ toxicity was also observed in $PM_{2.5}$-exposed or diesel exhaust particle-treated HUVECs, hippocampal neuron cells, bronchial epithelium cells, cornea, and conjunctiva human cell lines[4, 24, 35, 36, 37, 38]. After examining cell viability, treatments with $PM_{2.5}$ at concentrations of 100 and 200 μg/mL for 48 h were used for further mechanistic investigations, and the results were consistent with our *in vivo* observations, revealing increased levels of NLRP3, caspase-1, IL-1β, and GSDMD (Figure 1). The data show that after exposure of HTM cells to $PM_{2.5}$ for 48 h, the levels of these proteins increased (Figure 2B-E), suggesting that $PM_{2.5}$-induced HTM cell pyroptosis is the cellular mechanism underlying the development of ocular hypertension.

ROS generation can trigger NLRP3 inflammasome-associated protein production and inflammatory responses[4], and high ROS levels are detrimental to HTM cells and have been linked to ocular hypertension in glaucoma studies[34, 39]. In our study, a significant elevation of ROS was observed in HTM cells treated with 100 μg/mL $PM_{2.5}$ for 48 h (Figure 2F), along with enhanced HTM cell contractility (Figure 2G). HTM contractility is an important regulator of conductivity and decreases cell permeability and aqueous humor outflow by reducing the size of intercellular spaces, thereby promoting IOP elevation. In contrast, cell relaxation has the opposite effects[40]. The current observations indicate that oxidative stress damage induces HTM cell dysfunction through NLRP3-mediated pyroptosis.

NAC is a well-known ROS scavenger that decreases ROS production[41], while VX-765 is an effective selective inhibitor of caspase-1 with potent anti-inflammatory activity through inhibition of IL-1β and IL-18 release[42]. Previous studies also report that NAC can decreased ROS levels in HUVECs treated with cooking oil fume-derived $PM_{2.5}$ and downregulated NRLP3 expression[24]. Nicotine-induced atherosclerosis via ROS/NLRP3-mediated endothelial cell pyroptosis was also prevented by NAC and VX-765[43]. In our study, ROS scavenger NAC and caspase-1 inhibitor VX-765 were used to further verify the $PM_{2.5}$-related HTM cell injury mechanism. $PM_{2.5}$ at a concentration of 100 μg/mL was employed for further mechanistic experiments. Consistent with other studies, our results revealed that NAC (3 mM) or VX-765 (100 μM) pretreatment for 2 h improved HTM cell viability following $PM_{2.5}$ exposure (Figure 3A). NAC pretreatment efficiently reduced ROS levels and HTM contraction associated with $PM_{2.5}$ exposure (Figure S2, Figure 3F), inhibiting NLRP3, caspase-1, IL-1β, and GSDMD activation (Figure 3B-E). VX-765 pretreatment also resulted in relaxation of HTM cells following $PM_{2.5}$-induced contraction (Figure 3F) and inhibited caspase-1-mediated pyroptosis (Figure 3B-E). Hence, these results indicate that the $PM_{2.5}$ exposure elevated oxidative stress, which partially enhanced HTM cell contraction and contributed to an increase in IOP and activation of NLRP3/caspase-1/ IL-1β signaling. These *in vitro* observations support results from experiments in mice where elevated IOP was observed following $PM_{2.5}$ exposure, in parallel to oxidative stress damage and NLRP3/caspase-1-mediated pyroptosis. NAC and VX-765 administration

is, therefore, a potential therapeutic strategy for handling $PM_{2.5}$-induced high intraocular pressure disease.

There is a limitation to our study that we were not able to collect enough $PM_{2.5}$ samples for fine particulate matter components analysis. At the same location our group analyzed the $PM_{2.5}$ components and found elevated amounts of polycyclic aromatic hydrocarbons (PAHs)[44]. Future study should investigate the effect of major $PM_{2.5}$ components and the role of each one in the pathological process of $PM_{2.5}$-induced ocular hypertension.

Conclusion

This study provides novel evidence of the $PM_{2.5}$-mediated development of ocular hypertension, which occurs as a result of increased oxidative stress and the subsequent induction of pyroptosis in trabecular meshwork cells, key regulators of IOP. ROS scavenger and caspase-1 inhibitor effectively protected against the $PM_{2.5}$-induced damages.

Materials And Methods

Airborne particulate matter ($PM_{2.5}$) collection

Atmospheric $PM_{2.5}$ samples were obtained from January to October 2016 in Lanzhou, China, according to our previously described methods[44]. PM samples were gathered on glass fiber filters by a flow air particle sampler (TH-150C, Wuhan Tianhong Instrument Factory, Wuhan, China) at a constant flow rate of 100 L/min. The filter membranes were then cut into 1 cm x 1 cm squares and extracted three times using an ultrasonic extractor at 100 W for 15 min in deionized water. Next, each sample suspension was filtered using 12 gauze layers, and dried by a vacuum freeze-drying machine (Labconco, Kansas, USA). $PM_{2.5}$ samples were stored at −80°C, followed by resuspension of the resulting pellets in phosphate-buffered saline (PBS) before use.

Animals

C57BL/6 mice (3-4 weeks old) were purchased from the Shanghai Sippr-BK Laboratory Animal Co. Ltd. Mice were housed in clear cages loosely covered with air filters and containing a corncob pad as bedding. After a week of acclimatization, $PM_{2.5}$ suspension was topically applied to the right corneas of mice.

Fluorescent mock $PM_{2.5}$ particle tracing experiment

The fluorescent mock $PM_{2.5}$ particles prepared from SiO_2 (diameter: 10—500 nm) were a gift from Prof. Yonghui Deng at Fudan University. Particles were re-dissolved in PBS and topically applied to the eyes of mice. Frozen sections were prepared, and particle distribution was observed under a confocal fluorescence microscope (Leica).

$PM_{2.5}$ suspension topical exposure

Exposures were performed using a 1 mg/mL solution thrice daily (3 x 2 µL drops) over 3 months, with PBS applied topically to the contralateral eye as control. After 3 months, the mice were sacrificed, and outflow tissues were isolated and collected. All experiments complied with the Association for Research in Vision and Ophthalmology Statement on the use of animals in ophthalmic and vision research and were performed under the guidance of the Animal Care and Use Committee of Fudan University (Shanghai, China).

Mice IOP measurements

The IOP for both eyes was measured without anesthesia by rebound tonometry (TonoLab; ICare, Espoo, Finland). IOP was measured three times, and the average was used as the final value.

Western blotting

Mouse outflow tissue and HTM cells were lysed with a RIPA solution (Beyotime, Shanghai, China), and the protein concentration was determined by the BCA method (Beyotime, Shanghai, China). About 5–20 µg of protein were loaded onto gels and separated by SDS-PAGE (10% or 12% acrylamide). Proteins were then transferred onto polyvinylidene fluoride membranes (PVDF, 0.45 µm; Millipore, Shanghai, China) by electrophoresis. Membranes were blocked with 5 % non-fat dry milk for 2 hours at room temperature. PVDF membranes were probed with a primary antibody (dilutions of the primary antibodies are presented in Table 1), followed by incubation with peroxidase-conjugated secondary antibodies. Glyceraldehyde 3-phosphate dehydrogenase (GAPDH) was used as a loading control.

HTM cell culture and $PM_{2.5}$ treatment

HTM cells were purchased from ScienCell Research Laboratories (Shanghai, China). HTM cells were incubated in Trabecular Meshwork Cell Medium (ScienCell, Cat. No. 6591) containing 2% fetal bovine serum (FBS, Cat. No. 0010), 1% HTM growth supplement (TMCGS, Cat. No. 6592), and 1% penicillin/streptomycin (P/S, Cat. No. 0503) at 37°C and 5% CO_2.

For the experiments, HTM cells were seeded at a concentration of 5 x 10^5 cells/well in 6-well plates and 5 x 10^3 or 5 x 10^6 cells/well in 96-well plates. After cell attachment, the culture medium was replaced with fresh medium containing a $PM_{2.5}$ suspension or an equal volume of medium as a control. ROS scavenger acetylcysteine (N-Acetyl-L-cysteine, NAC, Sigma, Shanghai, China) 3 mM or caspase-1 inhibitor belnacasan (VX-765, Selleck, Shanghai, China) 100 uM were used. All experiments were performed at least three times.

Cell viability test

The viability of the $PM_{2.5}$-treated HTM cells was tested using a cell counting kit-8 (CCK-8) assay (Dojindo, Kumamoto, Japan) according to the manufacturer's instructions. Briefly, 100 µL of HTM

suspensions (5000 cells/well) were added into the wells of a 96-well plate and incubated until cell adhesion. CCK-8 solution (1:10) was then added to each well of the plate 2 h before measurement. The optical density (OD) was measured at 450 nm using a microplate reader (Tecan, Männedorf, Switzerland), and cell viability was reported as a percentage of the optical density values from unexposed control cells (100%).

Contractility assay and treatments

Collagen gels were prepared in 96-well plates from a collagen solution (1.85 mg/ml, Cell Biolabs, Beijing, China) by following the manufacturer's instructions. Briefly, HTM-containing medium (4 x 10^6 cells/mL) was added onto the collagen gel and incubated for 1 h at 37°C with 5% CO_2. After collagen polymerization, culture medium was added to each collagen gel lattice. Following a 48-h incubation, the edge of the gel was gently detached using a pipette tip. The gel area was then imaged using a Fluorescent Stereomicroscope (Leica M165 FC) every hour for 15 h in order to determine the time required for cessation of the "natural contraction" of the gel by HTM cells. Drugs (NAC or VX-765) were added to the medium, and images were captured at 6, 24, and 48 h. The gel area was calculated using the Fluorescent Stereomicroscope.

Reactive oxygen species generation detection

The intracellular ROS levels were detected by the Reactive Oxygen Species Assay Kit (ROS Assay Kit), following the manufacturer's instructions (Beyotime, Shanghai, China). HTM cells were washed with DMEM/F12 and were then treated with 2',7'-dichlorodihydrofluorescein diacetate (DCFH-DA, 1:1000, diluted by DMEM/F12) at 37°C for 20 min. After washing 3 times with the medium without FBS, the DCF fluorescence distribution of cells was detected. Rosup 50 μg/mL and 500 μg/mL were employed as the negative and positive control, respectively. The DCF fluorescence distribution of cells was observed under a fluorescence microscope (ZEISS, Shanghai, China).

RNA isolation and quantitative real-time polymerase chain reaction (qRT-PCR)

HTM cells were exposed to $PM_{2.5}$ (100 μg/mL and 200 μg/mL) for 48 h, while control cells were treated with PBS. Total RNA was then extracted using an RNeasy Mini Kit (Qiagen, Valencia, CA), and RNA concentration was measured by a NanoDrop 2000 spectrophotometer (Thermo Scientific, Wilmington, DE). mRNA expression was measured using the SYBR Green quantitative real-time PCR kit (qRT-PCR, Takara, Osaka, Japan) according to the manufacturer's instructions. Samples were amplified in a ViiA 7 Real-Time PCR System (Life Technologies, Pleasanton, CA), and mRNA expression was normalized to β-actin (the housekeeping gene). Expression was estimated using the comparative CT method ($2^{-\Delta\Delta CT}$) of relative quantification with the ViiA 7 Software (Life Technologies). Three independent experiments were conducted. The primer sequences used for the qRT-PCR are presented in Table 2.

Enzyme-linked immunosorbent assay (ELISA)

The IL-1β protein levels in the HTM cell culture medium were quantified using the human IL-1β ELISA kit (Abcam, Boston, MA) following the manufacturer's instructions. The optical density (OD) was read at 450 nm using a microplate reader (Tecan, Männedorf, Switzerland).

Immunofluorescence

Immunofluorescence analysis was performed using specific primary antibodies against NLRP3 (1:100, Abcam, Boston, USA) and caspase-1 (1:50, Proteintech, Shanghai, China). HTM cells grown on coverslips were fixed in 4% paraformaldehyde for 30 min at room temperature and were then washed three times with PBS. Cells were then treated with 0.1% Triton X-100 (Biotech Well, Shanghai, China) in PBS for 10 min and were once again washed three times. This was followed by blocking in PBS containing 0.5% bovine serum albumin (BSA, Roche, Shanghai, China) for 1 h at room temperature in a humidified chamber. The coverslips were then incubated with a primary antibody (dilutions of the primary antibodies are presented in Table 1) diluted in PBS containing 0.5% BSA overnight at 4°C in a humidified chamber. The cells were then washed three times with PBS and incubated with Alexa Fluor®555 anti-rabbit IgG (H+L) (1:200; donkey polyclonal; Beyotime, Shanghai, China) for 1 h at room temperature. After further washing with PBS, coverslips were stained with DAPI and stored at 4°C in the dark before being viewed under a confocal fluorescence microscope (Leica).

Statistics

The results are presented as the mean ± standard deviation (SD) or mean ± standard error of mean (SEM). Data were analyzed using SPSS 21.0 (IBM, Chicago, IL, USA). For normally distributed data, the paired t-test, independent t-test, or the Student's t-test were used for two-level comparisons, while one-way analysis of variance (ANOVA) was used for ≥ 3-level comparison. The Mann-Whitney U test was used for two-level comparisons, while the Kruskal-Wallis H test was used for ≥ 3-level comparisons of non-normally distributed data. In all cases, differences were considered significant at $p < 0.05$.

Abbreviations

PM: Particulate matter; IOP: intraocular pressure; HTM: Human trabecular meshwork; ROS: Reactive oxygen species; JCT: juxtacanalicular tissue; TM: Trabecular meshwork; SC: Schlemm's canal; NAC: N-Acetyl-L-cysteine; VX-765: Belnacasan; CCK-8: Cell counting kit-8.

Declarations

Availability of data and materials

The datasets during and/or analysed during the current study available from the corresponding author on reasonable request.

Ethical Approval and Consent to participate

All experiments complied with the Association for Research in Vision and Ophthalmology Statement on the use of animals in ophthalmic and vision research and were performed under the guidance of the Animal Care and Use Committee of Fudan University (Shanghai, China).

Consent for publication

Not applicable.

Availability of data and materials

The datasets during and/or analysed during the current study available from the corresponding author on reasonable request.

Competing interests

The authors declare that they have no competing interests.

Funding

This work was supported by BrightFocus Foundation (G2018112), National Science Foundation China (81100662, 81371015), Shanghai Municipal Health Bureau Young Outstanding Scientist Program (XYQ2013083), 211 Project of Fudan University (EHF158351), Scientific Research Foundation for the Returned Overseas Chinese Scholars (State Education Ministry), the International Science and Technology Cooperation Program of China (No.2015DFA31340), the National Natural Science Foundation of China (81872578).

Authors' contributions

Y.R, Y.L and H.S designed and supervised all the experiment work. L.L and C.X (contributed equally) acquired and analyzed the data used in the present study with assistance from L.N, B.L, J.Z, M.S, C.H, J.N. All authors contributed to the writing of the manuscript. And all authors read and approved the final manuscript.

Acknowledgments

The authors thank Prof. Yonghui Deng at Fudan University for the generous gift of the fluorescent mock $PM_{2.5}$ particles. We also thank Jianguo Sun, Ping Xu, Rong Zhang and Jufang Shi for her excellent assistance with the animal work.

Author's information

Liping Li[1], Chao Xing[2*], Liangliang Niu[1], Bin Luo[3,4] , Ji Zhou[5], Maomao Song[1], Jingping Niu [3],* Ye Ruan *[3#], Xinghuai Sun[1,6,7#], Yuan Lei[1,6#]*

[1]Department of Ophthalmology & Visual Science, Eye Institute, Eye & ENT Hospital, Shanghai Medical College, Fudan University, Shanghai 200031, China

[2]Experimental Research Center, Eye & ENT Hospital, Shanghai Medical College, Fudan University, Shanghai 200031, China

[3]Institute of Occupational Health and Environmental Health, School of Public Health, Lanzhou University, Lanzhou 730000, Gansu, China

[4]Shanghai Key Laboratory of Meteorology and health, Shanghai, 200030, China.

[5] Shanghai Key Laboratory of Meteorology and Health, Shanghai Meteorological Bureau, Shanghai, China

[6]Key Laboratory of Myopia, Chinese Academy of Medical Sciences (Fudan University), and Shanghai Key Laboratory of Visual Impairment and Restoration (Fudan University), Shanghai 200031, China

[7]State Key Laboratory of Medical Neurobiology, Institutes of Brain Science and Collaborative Innovation Center for Brain Science, Fudan University, Shanghai 200032, China

References

1. Chu C, Zhang H, Cui S, Han B, Zhou L, Zhang N, et al. Ambient PM2.5 caused depressive-like responses through Nrf2/NLRP3 signaling pathway modulating inflammation. J Hazard Mater. 2019;369:180-90; doi: 10.1016/j.jhazmat.2019.02.026. https://www.ncbi.nlm.nih.gov/pubmed/30776601.
2. Fuller R, Rahona E, Fisher S, Caravanos J, Webb D, Kass D, et al. Pollution and non-communicable disease: time to end the neglect. Lancet Planet Health. 2018;2 3:e96-e8; doi: 10.1016/S2542-5196(18)30020-2. https://www.ncbi.nlm.nih.gov/pubmed/29615229.
3. Mimura T, Ichinose T, Yamagami S, Fujishima H, Kamei Y, Goto M, et al. Airborne particulate matter (PM2.5) and the prevalence of allergic conjunctivitis in Japan. Sci Total Environ. 2014;487:493-9; doi: 10.1016/j.scitotenv.2014.04.057. https://www.ncbi.nlm.nih.gov/pubmed/24802272.
4. Tau J, Novaes P, Matsuda M, Tasat DR, Saldiva PH, Berra A. Diesel exhaust particles selectively induce both proinflammatory cytokines and mucin production in cornea and conjunctiva human cell lines. Invest Ophthalmol Vis Sci. 2013;54 7:4759-65; doi: 10.1167/iovs.12-10541. https://www.ncbi.nlm.nih.gov/pubmed/23722391.
5. Chang CJ, Yang HH, Chang CA, Tsai HY. Relationship between air pollution and outpatient visits for nonspecific conjunctivitis. Invest Ophthalmol Vis Sci. 2012;53 1:429-33; doi: 10.1167/iovs.11-8253. https://www.ncbi.nlm.nih.gov/pubmed/22205603.
6. Mimura T, Yamagami S, Fujishima H, Noma H, Kamei Y, Goto M, et al. Sensitization to Asian dust and allergic rhinoconjunctivitis. Environ Res. 2014;132:220-5; doi: 10.1016/j.envres.2014.04.014.

https://www.ncbi.nlm.nih.gov/pubmed/24815334.

7. Nwanaji-Enwerem JC, Wang W, Nwanaji-Enwerem O, Vokonas P, Baccarelli A, Weisskopf M, et al. Association of Long-term Ambient Black Carbon Exposure and Oxidative Stress Allelic Variants With Intraocular Pressure in Older Men. JAMA Ophthalmol. 2018; doi: 10.1001/jamaophthalmol.2018.5313. https://www.ncbi.nlm.nih.gov/pubmed/30419128.
8. Chua SYL, Khawaja AP, Dick AD, Morgan J, Dhillon B, Lotery AJ, et al. Ambient Air Pollution Associations with Retinal Morphology in the UK Biobank. Investigative Ophthalmology & Visual Science. 2020;61 5:32-; doi: 10.1167/iovs.61.5.32. https://doi.org/10.1167/iovs.61.5.32.
9. Chua SYL, Khawaja AP, Morgan J, Strouthidis N, Reisman C, Dick AD, et al. The Relationship Between Ambient Atmospheric Fine Particulate Matter (PM2.5) and Glaucoma in a Large Community Cohort. Investigative Ophthalmology & Visual Science. 2019;60 14:4915-23; doi: 10.1167/iovs.19-28346. https://doi.org/10.1167/iovs.19-28346.
10. Stamer WD, Braakman ST, Zhou EH, Ethier CR, Fredberg JJ, Overby DR, et al. Biomechanics of Schlemm's canal endothelium and intraocular pressure reduction. Prog Retin Eye Res. 2015;44:86-98; doi: 10.1016/j.preteyeres.2014.08.002. https://www.ncbi.nlm.nih.gov/pubmed/25223880.
11. Dong S, Shen X, Xia Z, Li X, Pan Q, Zhao Q. Changes in the epidemic of pulmonary tuberculosis in Shanghai from 1992 to 2016. Trop Med Int Health. 2018; doi: 10.1111/tmi.13187. https://www.ncbi.nlm.nih.gov/pubmed/30506617.
12. Sacca SC, Gandolfi S, Bagnis A, Manni G, Damonte G, Traverso CE, et al. From DNA damage to functional changes of the trabecular meshwork in aging and glaucoma. Ageing Res Rev. 2016;29:26-41; doi: 10.1016/j.arr.2016.05.012. https://www.ncbi.nlm.nih.gov/pubmed/27242026.
13. Schroder K, Tschopp J. The inflammasomes. Cell. 2010;140 6:821-32; doi: 10.1016/j.cell.2010.01.040. https://www.ncbi.nlm.nih.gov/pubmed/20303873.
14. Lamkanfi M, Dixit VM. Inflammasomes and their roles in health and disease. Annu Rev Cell Dev Biol. 2012;28:137-61; doi: 10.1146/annurev-cellbio-101011-155745. https://www.ncbi.nlm.nih.gov/pubmed/22974247.
15. Zheng Q, Ren Y, Reinach PS, She Y, Xiao B, Hua S, et al. Reactive oxygen species activated NLRP3 inflammasomes prime environment-induced murine dry eye. Exp Eye Res. 2014;125:1-8; doi: 10.1016/j.exer.2014.05.001. https://www.ncbi.nlm.nih.gov/pubmed/24836981.
16. Xiao Y, Xu W, Su W. NLRP3 inflammasome: A likely target for the treatment of allergic diseases. Clin Exp Allergy. 2018;48 9:1080-91; doi: 10.1111/cea.13190. https://www.ncbi.nlm.nih.gov/pubmed/29900602.
17. Zheng Q, Ren Y, Reinach PS, Xiao B, Lu H, Zhu Y, et al. Reactive oxygen species activated NLRP3 inflammasomes initiate inflammation in hyperosmolarity stressed human corneal epithelial cells and environment-induced dry eye patients. Exp Eye Res. 2015;134:133-40; doi: 10.1016/j.exer.2015.02.013. https://www.ncbi.nlm.nih.gov/pubmed/25701684.
18. Fan F, Wang S, Zhang Y, Xu D, Jia J, Li J, et al. Acute Effects of High-Level PM2.5 Exposure on Central Blood Pressure. Hypertension. 2019;74 6:1349-56; doi:

10.1161/HYPERTENSIONAHA.119.13408. https://www.ncbi.nlm.nih.gov/pubmed/31630576.

19. Dielemans I, Vingerling JR, Algra D, Hofman A, Grobbee DE, de Jong PT. Primary open-angle glaucoma, intraocular pressure, and systemic blood pressure in the general elderly population. The Rotterdam Study. Ophthalmology. 1995;102 1:54-60; doi: 10.1016/s0161-6420(95)31054-8. https://www.ncbi.nlm.nih.gov/pubmed/7831042.
20. Mozaffarieh M, Grieshaber MC, Flammer J. Oxygen and blood flow: players in the pathogenesis of glaucoma. Mol Vis. 2008;14:224-33. https://www.ncbi.nlm.nih.gov/pubmed/18334938.
21. Guzik TJ, Touyz RM. Oxidative Stress, Inflammation, and Vascular Aging in Hypertension. Hypertension. 2017;70 4:660-7; doi: 10.1161/HYPERTENSIONAHA.117.07802. https://www.ncbi.nlm.nih.gov/pubmed/28784646.
22. McMonnies C. Reactive oxygen species, oxidative stress, glaucoma and hyperbaric oxygen therapy. J Optom. 2018;11 1:3-9; doi: 10.1016/j.optom.2017.06.002. https://www.ncbi.nlm.nih.gov/pubmed/28760643.
23. Duan S, Wang N, Huang L, Zhao Y, Shao H, Jin Y, et al. NLRP3 inflammasome activation is associated with PM2.5 -induced cardiac functional and pathological injury in mice. Environ Toxicol. 2019;34 11:1246-54; doi: 10.1002/tox.22825. https://www.ncbi.nlm.nih.gov/pubmed/31313453.
24. Shen C, Liu J, Zhu F, Lei R, Cheng H, Zhang C, et al. The effects of cooking oil fumes-derived PM2.5 on blood vessel formation through ROS-mediated NLRP3 inflammasome pathway in human umbilical vein endothelial cells. Ecotoxicol Environ Saf. 2019;174:690-8; doi: 10.1016/j.ecoenv.2019.03.028. https://www.ncbi.nlm.nih.gov/pubmed/30878009.
25. Pavillard LE, Marin-Aguilar F, Bullon P, Cordero MD. Cardiovascular diseases, NLRP3 inflammasome, and western dietary patterns. Pharmacol Res. 2018;131:44-50; doi: 10.1016/j.phrs.2018.03.018. https://www.ncbi.nlm.nih.gov/pubmed/29588192.
26. Liu D, Zeng X, Li X, Mehta JL, Wang X. Role of NLRP3 inflammasome in the pathogenesis of cardiovascular diseases. Basic Res Cardiol. 2018;113 1:5; doi: 10.1007/s00395-017-0663-9. https://www.ncbi.nlm.nih.gov/pubmed/29224086.
27. Eren E, Ozoren N. The NLRP3 inflammasome: a new player in neurological diseases. Turk J Biol. 2019;43 6:349-59; doi: 10.3906/biy-1909-31. https://www.ncbi.nlm.nih.gov/pubmed/31892810.
28. Kopalli SR, Kang TB, Lee KH, Koppula S. NLRP3 Inflammasome Activation Inhibitors in Inflammation-Associated Cancer Immunotherapy: An Update on the Recent Patents. Recent Pat Anticancer Drug Discov. 2018;13 1:106-17; doi: 10.2174/1574892812666171027102627. https://www.ncbi.nlm.nih.gov/pubmed/29076433.
29. Li F, Xu M, Wang M, Wang L, Wang H, Zhang H, et al. Roles of mitochondrial ROS and NLRP3 inflammasome in multiple ozone-induced lung inflammation and emphysema. Respir Res. 2018;19 1:230; doi: 10.1186/s12931-018-0931-8. https://www.ncbi.nlm.nih.gov/pubmed/30466433.
30. Faner R, Sobradillo P, Noguera A, Gomez C, Cruz T, Lopez-Giraldo A, et al. The inflammasome pathway in stable COPD and acute exacerbations. ERJ Open Res. 2016;2 3; doi: 10.1183/23120541.00002-2016. https://www.ncbi.nlm.nih.gov/pubmed/27730204.

31. Zhuang J, Cui H, Zhuang L, Zhai Z, Yang F, Luo G, et al. Bronchial epithelial pyroptosis promotes airway inflammation in a murine model of toluene diisocyanate-induced asthma. Biomed Pharmacother. 2020;125:109925; doi: 10.1016/j.biopha.2020.109925. https://www.ncbi.nlm.nih.gov/pubmed/32014690.
32. Gaidt MM, Hornung V. The NLRP3 Inflammasome Renders Cell Death Pro-inflammatory. J Mol Biol. 2018;430 2:133-41; doi: 10.1016/j.jmb.2017.11.013. https://www.ncbi.nlm.nih.gov/pubmed/29203171.
33. Miao EA, Rajan JV, Aderem A. Caspase-1-induced pyroptotic cell death. Immunol Rev. 2011;243 1:206-14; doi: 10.1111/j.1600-065X.2011.01044.x. https://www.ncbi.nlm.nih.gov/pubmed/21884178.
34. Llobet A, Gasull X, Gual A. Understanding trabecular meshwork physiology: a key to the control of intraocular pressure? News Physiol Sci. 2003;18:205-9; doi: 10.1152/nips.01443.2003. https://www.ncbi.nlm.nih.gov/pubmed/14500801.
35. Li B, Guo L, Ku T, Chen M, Li G, Sang N. PM2.5 exposure stimulates COX-2-mediated excitatory synaptic transmission via ROS-NF-kappaB pathway. Chemosphere. 2018;190:124-34; doi: 10.1016/j.chemosphere.2017.09.098. https://www.ncbi.nlm.nih.gov/pubmed/28987401.
36. Fu Q, Lyu D, Zhang L, Qin Z, Tang Q, Yin H, et al. Airborne particulate matter (PM2.5) triggers autophagy in human corneal epithelial cell line. Environ Pollut. 2017;227:314-22; doi: 10.1016/j.envpol.2017.04.078. https://www.ncbi.nlm.nih.gov/pubmed/28477555.
37. Yang Q, Li K, Li D, Zhang Y, Liu X, Wu K. Effects of fine particulate matter on the ocular surface: An in vitro and in vivo study. Biomed Pharmacother. 2019;117:109177; doi: 10.1016/j.biopha.2019.109177. https://www.ncbi.nlm.nih.gov/pubmed/31387168.
38. Zhu XM, Wang Q, Xing WW, Long MH, Fu WL, Xia WR, et al. PM2.5 induces autophagy-mediated cell death via NOS2 signaling in human bronchial epithelium cells. Int J Biol Sci. 2018;14 5:557-64; doi: 10.7150/ijbs.24546. https://www.ncbi.nlm.nih.gov/pubmed/29805307.
39. Liton PB. The autophagic lysosomal system in outflow pathway physiology and pathophysiology. Exp Eye Res. 2016;144:29-37; doi: 10.1016/j.exer.2015.07.013. https://www.ncbi.nlm.nih.gov/pubmed/26226231.
40. Luna C, Li G, Huang J, Qiu J, Wu J, Yuan F, et al. Regulation of trabecular meshwork cell contraction and intraocular pressure by miR-200c. PLoS One. 2012;7 12:e51688; doi: 10.1371/journal.pone.0051688. https://www.ncbi.nlm.nih.gov/pubmed/23272142.
41. Halasi M, Wang M, Chavan TS, Gaponenko V, Hay N, Gartel AL. ROS inhibitor N-acetyl-L-cysteine antagonizes the activity of proteasome inhibitors. Biochem J. 2013;454 2:201-8; doi: 10.1042/BJ20130282. https://www.ncbi.nlm.nih.gov/pubmed/23772801.
42. Wannamaker W, Davies R, Namchuk M, Pollard J, Ford P, Ku G, et al. (S)-1-((S)-2-{[1-(4-amino-3-chloro-phenyl)-methanoyl]-amino}-3,3-dimethyl-butanoy l)-pyrrolidine-2-carboxylic acid ((2R,3S)-2-ethoxy-5-oxo-tetrahydro-furan-3-yl)-amide (VX-765), an orally available selective interleukin (IL)-converting enzyme/caspase-1 inhibitor, exhibits potent anti-inflammatory activities by inhibiting the release of

IL-1beta and IL-18. J Pharmacol Exp Ther. 2007;321 2:509-16; doi: 10.1124/jpet.106.111344. https://www.ncbi.nlm.nih.gov/pubmed/17289835.

43. Wu X, Zhang H, Qi W, Zhang Y, Li J, Li Z, et al. Nicotine promotes atherosclerosis via ROS-NLRP3-mediated endothelial cell pyroptosis. Cell Death Dis. 2018;9 2:171; doi: 10.1038/s41419-017-0257-3. https://www.ncbi.nlm.nih.gov/pubmed/29416034.
44. Luo B, Shi H, Zhang K, Wei Q, Niu J, Wang J, et al. Cold stress provokes lung injury in rats co-exposed to fine particulate matter and lipopolysaccharide. Ecotoxicol Environ Saf. 2019;168:9-16; doi: 10.1016/j.ecoenv.2018.10.064. https://www.ncbi.nlm.nih.gov/pubmed/30384172.

Tables

Table 1: Primary antibodies used in the study

Antibody	Source	Catalog No	Type of Ab	Dilution	MW
NLRP3	Abcam	ab214185	Rabbit polyclonal	1:1000 (WB) 1:200 (IF)	114 kD
Caspase-1	Abcam	ab207802	Rabbit polyclonal	1:1000 (WB)	35, 70 kD
Caspase-1	CST	22915-1-AP	Rabbit polyclonal	1:200 (IF)	
IL-1β	Abcam	ab9722	Rabbit polyclonal	1:1000 (WB)	30, 45 kD
GSDMD	Abcam	ab215203	Rabbit monoclonal	1:1000 (WB)	35, 250 kD
GAPDH	Abcam	ab8245	Mouse monoclonal	1:1000 (WB)	36 kD

CST, Cell Signaling Technology; IF, immunofluorescence; MW, molecular weight; WB, western blotting.

Table 2: Primers used for RT-PCR

Gene	Primer
NLRP3	Forward: 5′-GCACTTGCTGGACCATCCTC-3′
	Reverse: 5′-GTCCAGTGCACACGATCCAG-3′
Caspase-1	Forward: 5′-AAGACCCGAGCTTTGATTGACTC-3′
	Reverse: 5′-AAATCTCTGCCGACTTTTGTTTCC-3′
IL-1β	Forward: 5′-TATTACAGTGGCAATGAGG-3′
	Reverse: 5′-ATGAAGGGAAAGAAGGTG-3′
β-actin	Forward: 5′-CCCTGGACTTCGAGCAAGAG -3′
	Reverse: 5′-TCACACTTCATGATGGAGTTG-3′

Figures

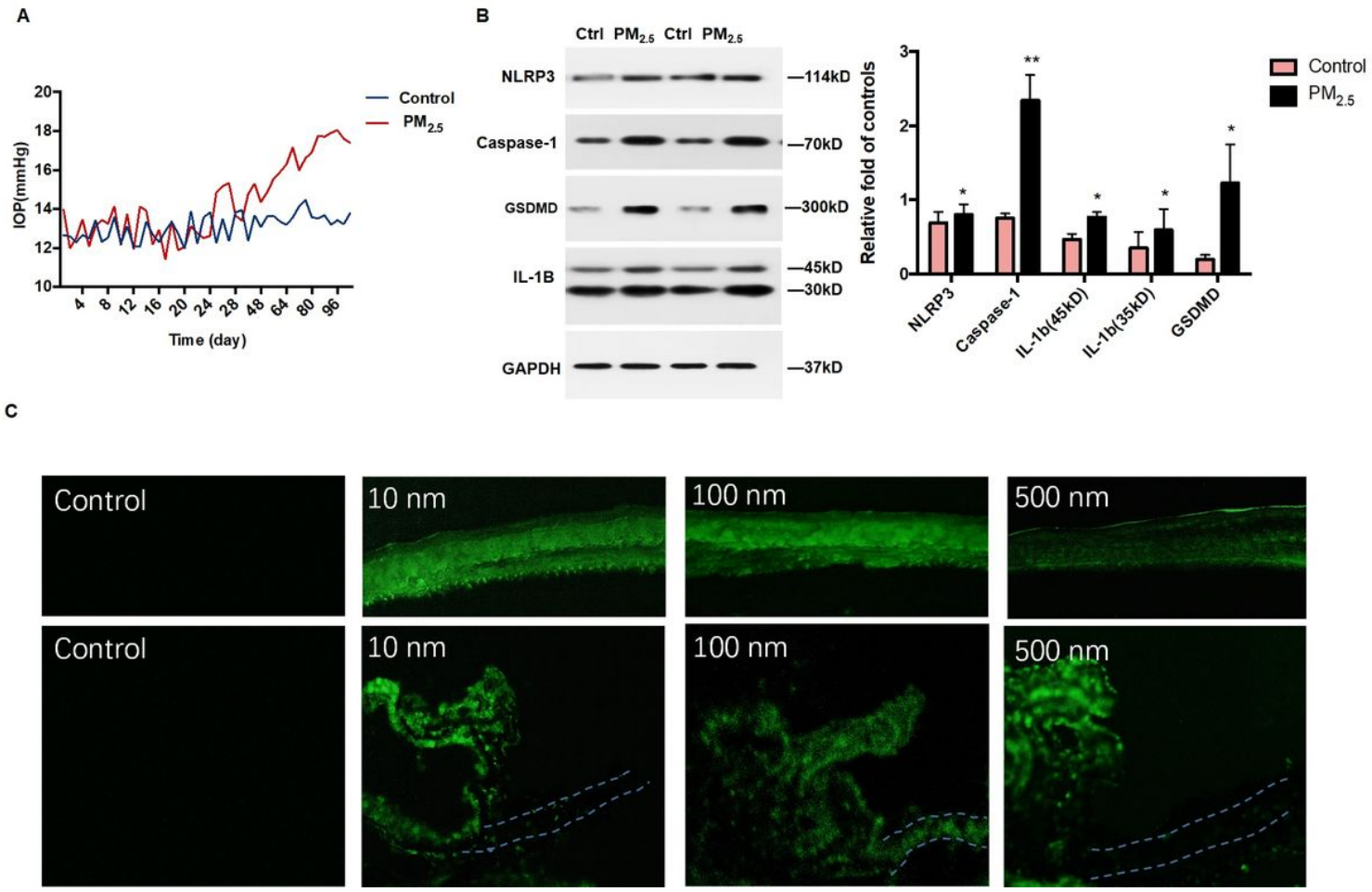

Figure 1

A. PM2.5 exposure induced ocular hypertension in C57BL/6 mice. The IOP was measured without anesthesia by rebound tonometry measurements and the results showed that the IOP was elevated gradually on the PM2.5-treated mice eyes compared with the control eyes ($n \geq 6$, independent sample t-test or Mann-Whitney U test). B. PM2.5 application increased the expressions of NLRP3 inflammasome-related proteins in mice outflow tissues. Relative protein expressions of NLRP3, caspase-1, GSDMD and IL-1β determined by western blot and showed in A-D ($n = 3, 4, 3, 3$, $*p < 0.05$, paired sample t-test). Date are represented as the mean ± standard deviation. Ctrl = PBS-treated control; PM2.5 = PM2.5 exposure. C, Fluorescent mock PM2.5 particles topically applied to the eye deposited in intraocular tissues. Particle diameter from 10 nm to 500 nm could pass through the cornea and enter the anterior chamber finally deposited mainly on the ciliary body. The dotted line shows the outline of the iris.

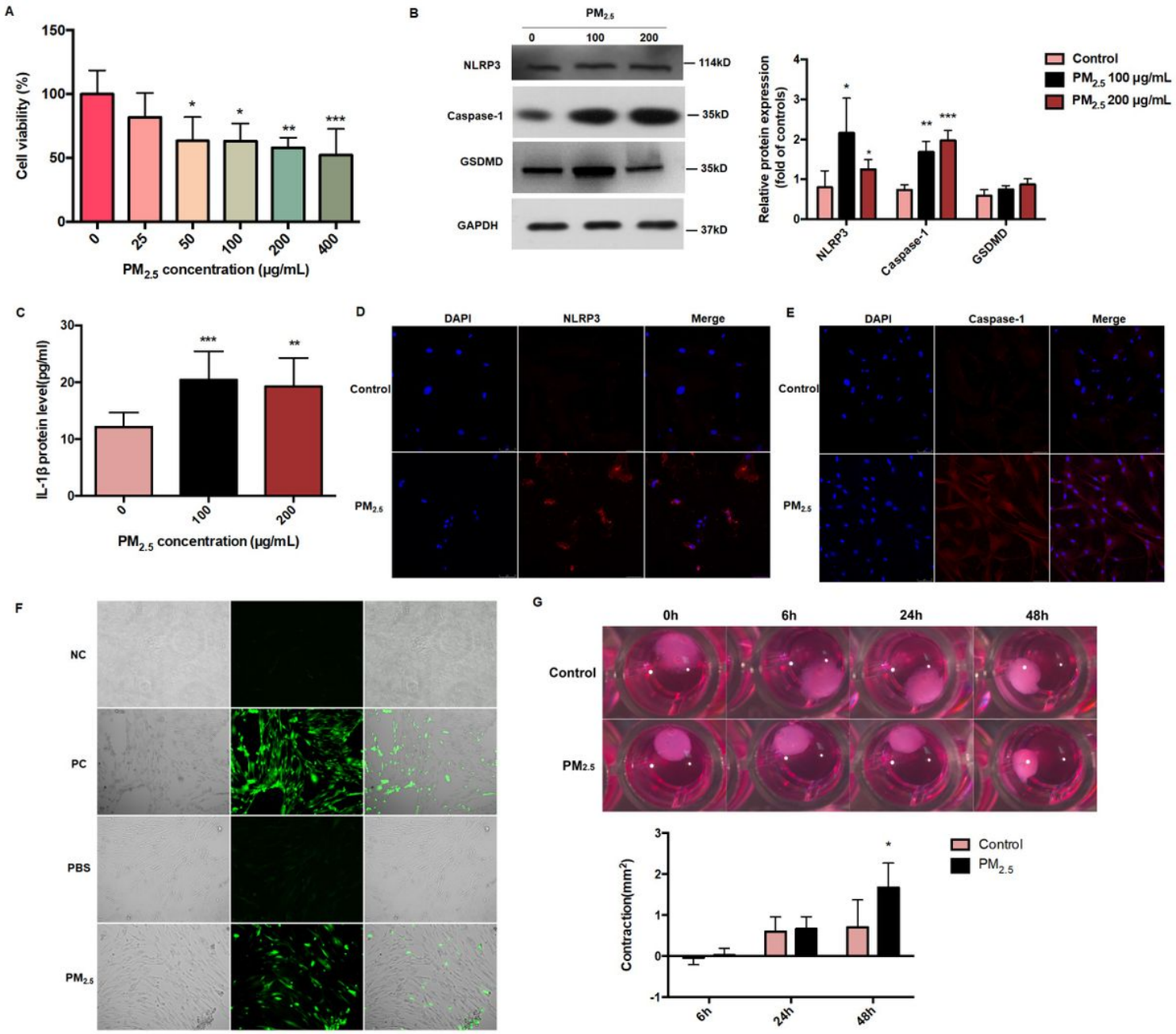

Figure 2

A, Effects of PM2.5-exposure on HTM cell viability. Cell viability were analyzed by cell viability assay (CCK-8). The human trabecular meshwork cells were treated with different concentrations of PM2.5 (0 μg/mL, 25 μg/mL, 25 μg/mL, 50 μg/mL, 100 μg/mL, 200 μg/mL, or 400 μg/mL) for 48 h. (n = 5 cell lines , *p < 0.05, **p < 0.01, ***p < 0.001, by one-way ANOVA, compared with the control). Date are represented as the mean ± standard deviation. B, C, Expressions of NLRP3 inflammasome-related proteins in PM2.5-treated TM cells. After HTM cells were treated by PM2.5 100 μg/mL or 200 μg/mL, relative protein expressions of NLRP3, caspase-1, and GSDMD determined by western blot and IL-1β by ELISA showed in B and C (n = 4, 3, 3, 8, *p < 0.05, one-way ANOVA, compared with the control). Date are represented as the mean ± standard deviation. D, E, immunofluorescence examination showed increased protein expressions

of NLRP3 and caspase-1 in HTM cells after PM2.5 exposure. Representative immunofluorescence images of the punctate staining of NLRP3 (E) and caspase-1 (F) in HTM cells treated with the vehicle control or PM2.5 100 μg/mL for 48 h. Blue, DAPI; red, NLRP3 (A) or caspase-1 (B). Magnification, 20X. F, ROS elevation in PM2.5-treated HTM cells. ROS fluorescence staining images of Rosup negative control (NC, 50 μg/mL), Rosup positive control (PC, 500 μg/mL , PBS control group (Control) and PM2.5 100 μg/mL group (PM2.5). ROS were detected by Reactive Oxygen Species Assay Kit. In each panel, from left to right are bright filed, fluorescence and merged image of fluorescence and bright field. HTM cells were treated with PM2.5 (100 μg/mL) for 48 h. ROS levels were significantly increased in HTM cells treated with Rosup positive control and 100 ug/ml PM2.5. Magnification, 10X. G, PM2.5 exposure impacted cell contraction in collagen gels. HTM cells were treated with PM2.5 (100 μg/mL) for 48 h. The cell contractility was detected in 6 h, 24 h, and 48 h by Contractility Assay. (n = 3 , *p < 0.05, **p < 0.01, ***p < 0.001, by Student' t test, compared with the control). Date are represented as the mean ± standard error of mean.

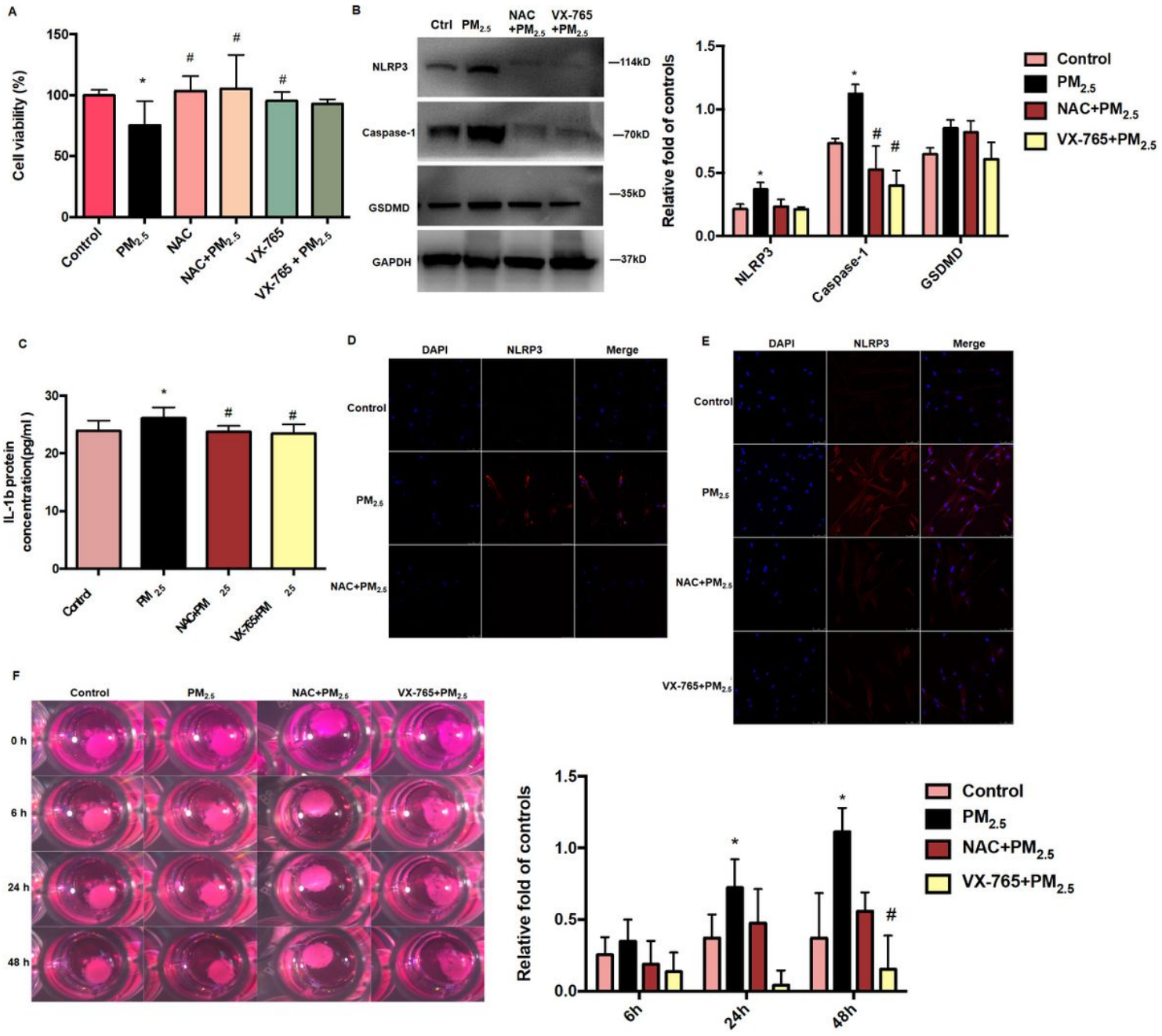

Figure 3

A Effects of PM2.5-exposure on HTM cell viability. Effects of NAC pretreatment (2 h) on PM2.5-exposed HTM cell viability. Cell viability was analyzed by cell viability assay (CCK-8). NAC pretreatment (2 h) improved HTM cell viability impaired by 100 μg/mL PM2.5 for 48 h (n = 5 cell lines, *p < 0.05, one-way ANOVA, compared with the control; #p < 0.05, one-way ANOVA, Compare with PM2.5 100 μg/mL). Date are represented as the mean ± standard deviation. B, C, NAC and VX-765 inhibited PM2.5 induced NLRP3 inflammasome activation. Relative protein expressions of NLRP3, caspase-1, GSDMD and IL-1 β , determined by western blot (B) and ELISA (C) (n = 3, 3, 3, 5, *p < 0.05, one-way ANOVA, compared with the control; #p < 0.05, one-way ANOVA, compare with PM2.5 100 μg/mL). Ctrl = PBS-treated control; PM2.5 = PM2.5 100 μg/mL; NAC + PM2.5 = NAC 3 mM pretreated 2 h + PM2.5 100 μg/mL; VX-765 + PM2.5 = VX-

765 100 uM pretreated 2 h + PM2.5100 μg/mL. Date are represented as the mean ± standard deviation. D, E, NAC or VX-765 downregulated NLRP3 associated proteins in HTM cells after PM2.5 exposure through immunofluorescence examination. Representative immunofluorescence images of the punctate staining of NLRP3 (E) and caspase-1 (F) in HTM cells treated with the vehicle control or PM2.5 100 μg/mL for 48 h, pretreated with or without NAC 3 mM or VX-765 100 μM for 2 h. Blue, DAPI; red, NLRP3 (E) or caspase-1 (F). Magnification, 20X. F, Effects of PM2.5-exposure on HTM cell contraction. HTM cell contraction were analyzed by Contractility Assay. NAC 3 mM or VX-765 100 μM pretreatment (2 h) resulted in strong inhibition of PM2.5-exposed HTM cell contraction in collagen populated gels. (n = 3, 4, 5 cell lines, *p < 0.05, one-way ANOVA, compared with the control; #p < 0.05, one-way ANOVA, Compare with PM2.5 100 μg/mL). Date are represented as the mean ± standard error of mean.

Supplementary Files

This is a list of supplementary files associated with this preprint. Click to download.

- Supplementary.docx